TELAC REPORT 90-19

COMPOSITE FUSELAGE TECHNOLOGY

Annual Report for period April 7, 1989 to April 6, 1990
on NASA Langley Research Grant NAG-1-991

Michael J. Graves and Paul A. Lagace
Assistant Professor Associate Professor

OCTOBER, 1990

Objectives

The overall objective of this work is to identify and understand, via directed experimentation and analysis, the mechanisms which control the structural behavior of fuselages in their response to damage (resistance, tolerance, and arrest). A further objective is to develop straightforward design methodologies which can be employed by structural designers in preliminary design stages to make intelligent choices concerning the material, layup, and structural configuration so that a more efficient structure with structural integrity can be designed and built.

General Approach

Although there are three different facets of the damage issue and these facets do interact, it is possible to first pursue these independently: damage resistance, damage tolerance, and damage arrest. This multiple year effort began with careful consideration of work available in the open literature on damage in general composite structures (e.g. Reference [2]) and damage specifically in fuselage-type structures made of composites (e.g. Reference [3]).

The initial work focused on damage growth and damage arrest. It has been shown [4] that the direction of damage propagation can be changed by the particular structural configuration of a pressurized composite cylinder. This indicates that a mechanism does exist by which the path of damage can be altered in composite construction. The next step is to fully arrest the damage. Before proceeding to this next step, the previously tested configurations of Reference 4 were structurally analyzed to determine the differences between them. Particular attention was paid to the stiffness and stress field as a function of the propagating damage in an attempt to

identify the mechanism(s) which redirect propagating damage. Once these mechanisms are identified, graphite/epoxy cylinders of various structural configurations will be designed which will isolate the identified mechanisms and thus allow further testing of the mechanisms.

From this work and the experimental and analytical results, rules of thumb for design will be formulated and further tested in experiment.

Work will later commence on the damage resistance and damage tolerance facets of the damage issue again looking at the same factors as previously mentioned utilizing similar experimental techniques. Damage will initially be introduced as through-cracks, but other types of damage will then be considered including delamination and other damage combinations which typically occur due to impact of other events. It is recognized that through-cracks do not represent realistic damage to composite structures in service. However, a through-crack is a well-defined damage state and will be used in the initial work to determine the important operative mechanisms in damage arrest. Once the mechanisms have been identified, the more realistic damage states will be considered.

In all cases through this ongoing multi-year effort, analysis will be used to guide the experimentation to isolate specific mechanisms and determine their effects on the damage issues. Initial analysis will continue to be accomplished using the finite element method and appropriate elements. Special shell elements utilizing the hybrid stress concept and developed in the laboratory [8] may be employed.

Once the mechanisms and parameters are identified, their effects as they are changed will be ascertained so as to determine design methodologies for composite fuselages. Of particular importance are scaling and structural tailoring. Whereas the finite element method is useful in the identification of mechanisms and in point design, emphasis will also be placed on developing more time-efficient analyses suitable for preliminary design stages. These analyses will incorporate the physics of the problem

determined through the earlier experimentation and analysis. It is intended that the analyses will thus give the designer a "feel" for the problem as well as allowing the designer to run a number of parametric studies so that the most effective design can be achieved. Without knowledge of the specific mechanisms involved, it is premature to comment on the exact form these analyses might take.

Year 1 Objectives

During the first year, the work concentrated on identifying the mechanisms by which damage paths can be altered and propagating damage arrested in pressurized composite cylinders. Once these mechanisms are identified, the effects of various configurations on this was investigated. This work was anticipated to continue, and is continuing, into the second year.

The specific work pursued during this first year to achieve these objectives was as follows. One, the stress/strain field as a function of propagating damage in pressurized fuselages was determined. Two, possible mechanisms and factors in the ability to change the direction of propagating damage were identified. Three, graphite/epoxy plates and cylinders were utilized to examine the mechanisms identified.

Summary of Work Completed in Year 1

Experimental Work

One possible mechanism identified as affecting the direction of propagation of damage was the local change in bending stiffness due to a stiffener placed ahead of the damage. Stiffened plates and cylinders with through-thickness slits perpendicular to the primary load direction were fabricated and tested to better understand this mechanism.

Plate Specimens

Nine stiffened plate specimens were fabricated and tested. The materials used and the layups are given in Table 1. Three stiffener layups and three crack lengths were included and are illustrated in Figure 1. Experimental results for stiffened plate specimens indicate no definable mechanism to alter damage propagation paths. All failures extended through the stiffeners to the edge of the specimen. The A type specimens exhibited damage propagation both along the 45° plies and perpendicular to loading. Their stiffener plies showed a tendency to disbond from fabric plies at failure. The B and C type specimens all exhibited damage propagation perpendicular to loading. These differences may be attributed to the bending-stretching coupling inherent in the non-symmetric A laminate layup. Failure loads are given in Table 1. Photoelastic coatings were placed on all specimens. Typical photoelastic data and computer-enhanced images for the plate specimens are compared to finite element predictions of strain intensity (difference of principal strains) in Figures 7 through 10.. The numeric magnitudes refer to the fringe order numbers of the photoelastic fringes.

Cylinder Specimens

Nine cylinder specimens were manufactured in an autoclave using techniques previously developed in the laboratory. The materials used and the layups are given in Table 2. Testing took place in a blast chamber where the cylinders were pressurized with nitrogen gas [5]. Three stiffener layups and three crack lengths were included. These are illustrated in Figure 2. The endcap system pictured in Figure 3 [6] was utilized. Strain gages were placed in appropriate locations to monitor important strain effects especially local bending which is important in the response of pressurized cylinders [7]. Specimen type and failure data are given in Table 2. All of the cylinders exhibited damage bifurcation, and all of the stiffened cylinders exhibited damage redirection upon reaching the stiffened regions. The unstiffened cylinder exhibited initial damage propagation in the axial direction. The damage then bifurcated and ran in the ±45° direction until it reached the endcaps. All of the stiffened cylinders exhibited damage bifurcation prior to reaching the stiffened regions. Upon reaching the stiffened regions, the bifurcated damage was redirected to the hoop direction and continued to run until pressure loads were sufficiently released. As shown in Figures 4 and 5, propagating damage in cylinders with stiffener types A and B bifurcated closer to the stiffened regions than damage in types C and D. Bifurcated damage in cylinder types A and B propagated along the boundary of the stiffened and the unstiffened regions. Bifurcated damage in cylinder types C and D propagated into the stiffened regions.

Analytical Work

Analytical work including finite element analysis has been initiated for both flat plate and cylinder specimens to identify possible mechanism and factors related to damage propagation. The specimens were modeled using ADINA [9], a displacement-based finite element code and run on a DEC MicroVAX. Eight node isoparametric elements were used to model the plates. Sixteen node isoparametric shell elements were used to model the cylinders. Limits of the finite element models can be summarized as follows: a) Unlike the plate models, the cylinder models do not contain special crack tip elements. Instead, the nodes are disconnected to model a crack; b) Neither model takes into account the stacking sequence of the laminates. The material properties are smeared through the thickness, so the differences in stiffener stacking sequence cannot be modeled; c) Neither model accounts for the unsymmetrical nature of manufactured plates and cylinders as illustrated in Figure 6.

Typical finite element results for the plate and cylinder specimens are shown in Figures 11 through 16. The finite element models seemed to predict the photoelastic behavior of plates that did not exhibit significant bending response to loading. Bending effects were not accounted for in the finite element models of the panels which exhibited significant bending- stretching coupling (the B and C type panels with short slits), so the models did not accurately predict their photoelastic behavior. The models, however, did predict the overall magnitudes of strain intensity of the photoelastic images. The contour patterns of the finite element models were consistent with the photoelastic patterns found in the photographs.

One interesting result to note for the plate analysis is that the orientation of the maximum tensile strain remains essentially perpendicular to the slit direction for the condition when the slit tip is very near the reinforcement. Also, the magnitude of the maximum tensile strain increases dramatically just ahead of the slit tip. Finite element

results for the cylinders indicate a markedly different response. Unlike the case of the plate, the reinforcement lowers the strain field ahead of the slit tip and further rotates the maximum strain orientation. Furthermore, for large slits, the orientation is no longer perpendicular to the slit direction with and without the reinforcement.

Preliminary Results

Preliminary results indicate the following conclusion for these quasi-isotropic fabric laminates: It is hypothesized that damage propagates perpendicular to a principal strain direction. In the case of the panels, the stiffeners do not redirect and arrest the damage and the analysis indicates that both the magnitude and orientation of the maximum strain correlate well with the experiment. In the case of the stiffened cylinders, damage bifurcates as the slit grows and redirects along the stiffener. This also correlates well with the analytical results. The conclusion reached is that the local strain field region ahead of the flaw is the controlling factor in subsequent damage propagation and thus in order to control the damage path, the proper structural configuration must be provided. Furthermore, the membrane as well as bending stiffness in this region must be accounted for in any structural analysis used to predict failure.

A master's thesis fully documenting the effort in year 1 is being completed.

Plans for Year 2

Initially during the second year, the work accomplished in year 1 will be fully documented in a Master's thesis. The work will then progress to further investigation of the mechanisms identified in Phase I and extensions of these results as the structural configuration is altered. It is hoped that this will culminate in the identification of structural configurations which will successfully arrest damage and which can be tested in the third year.

The analysis begun in Year 1 to better understand the phenomena observed in both the plates and cylinders will be continued. This includes more refined finite element models to account for stacking sequence and curing variations in both the plates and cylinders which were not incorporated in the initial analysis.

An experimental program to extend the testing to include the influence of radius of curvature and stacking sequence in the base laminate as well as stiffener configuration and material form on damage propagation will begin. In particular, base laminates using tape ($[\pm 45/0]_s$ and $[\pm 45/90]_s$) will be included to account for the failure modes and additional orthotropy of tape laminates. This information will be used to guide the formulation of a Phase III test program to further investigate the predictive capability of these models and allow for the creation and verification of analysis tools incorporating the effects determined to be important in the design of composite fuselages.

REFERENCES

1. *Advanced Organic Composite Materials for Aircraft Structures - Future Program*, Report of the National Research Council Committee on the Status and Viability of Composite Materials for Aircraft Structures, National Academy Press, Washington, D.C., 1987.

2. "Damage Tolerance of Composites", Final Government/Industry Review of USAF Contract F33615-82-C-3213, presented at Monterey, California, April, 1987.

3. P.A. Lagace and K.J. Saeger, "Damage Tolerance Characteristics of Pressurized Graphite/Epoxy Cylinders", *Proceedings of the Sixth International Symposium on Offshore Mechanics and Arctic Engineering*, ASME, Houston, Texas, March, 1987, pp. 31-37.

4. M.J. Graves and P.A. Lagace, "Damage Tolerance of Composite Cylinders", *Composite Structures*, Vol. 4, No.1, 1985, pp. 75-91.

5. K.J. Saeger and P.A. Lagace, "Fracture of Pressurized Composite Cylinders with a High Strain-to-Failure Matrix System", Composite Materials: *Fatigue and Fracture, Second Volume, ASTM STP 1012*, ASTM, Philadelphia, 1989, pp. 326-337.

6. M.J. Kraft, "Impact Damage Response of Graphite/Epoxy Fabric Structures", TELAC Report 88-9, Massachusetts Institute of Technology, July, 1988.

7. E.S. Folias, "Asymptotic Approximation to Crack Problems in Shells", Mechanics of Fracture, Vol. 3, Noordhogg International, Leiden, the Netherlands, 1977, pp. 117-160.

8. K. Sumihara, "Thin Shell and New Invariant Elements by Hybrid Stress Method", Ph.D. Thesis, Massachusetts Institute of Technology, June, 1983.

9. "Automatic Dynamic Incremental Nonlinear Analysis-Input:User's Manual," Report ARD 87-4, ADINA R. & D., Inc., 1987.

Figure 1 Physical Characteristics of the Plate Specimens

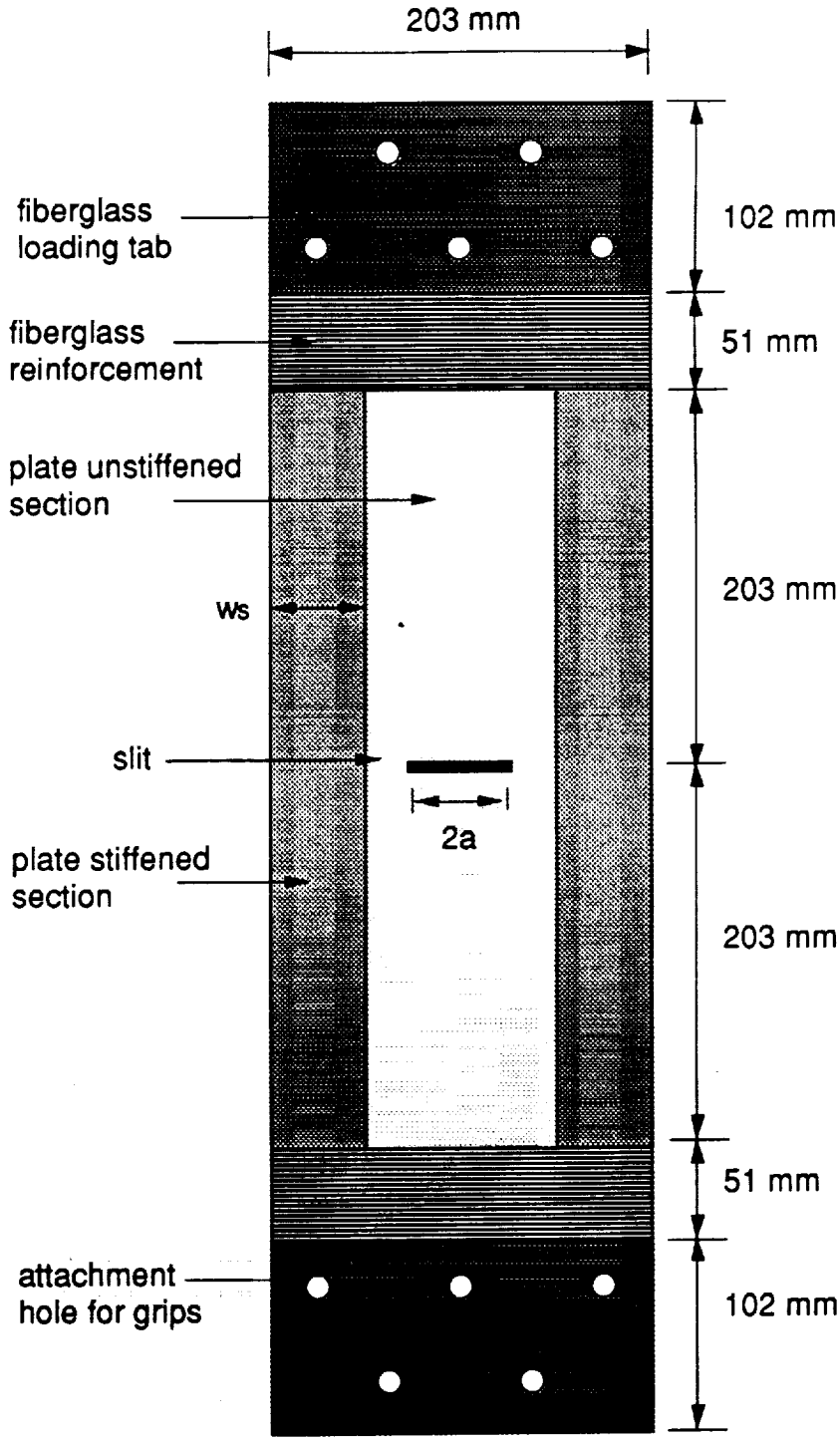

2a = width of slit

ws = width of stiffeners after milling

Figure 2 Physical Characteristics of the Cylinder Specimens

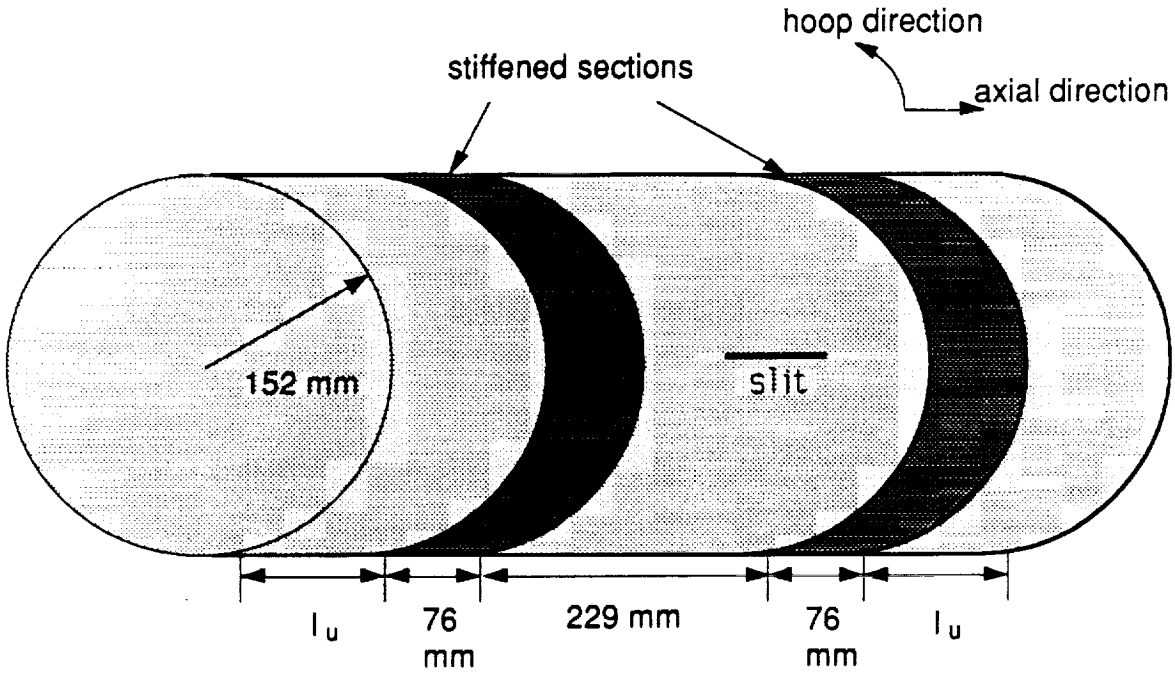

l_u = distance between end of cylinder and stiffener
= 165 mm for cylinder number 8
= 114 mm for all other cylinders

Figure 3 Endcap System for Cylinder Specimen

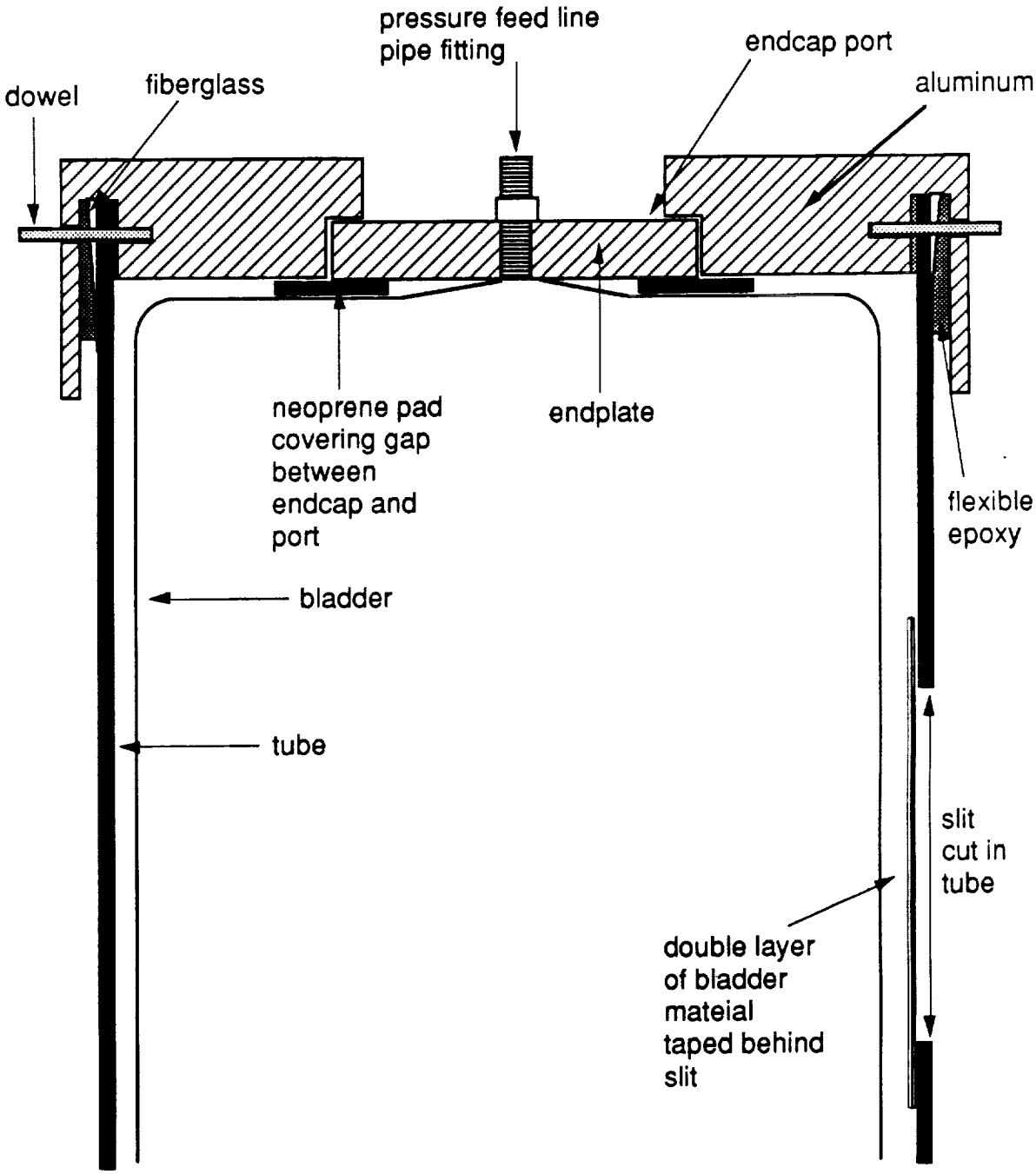

Figure 4 Schematic of damage propagation paths in cylinders types A, B, and C with 102 mm long slits

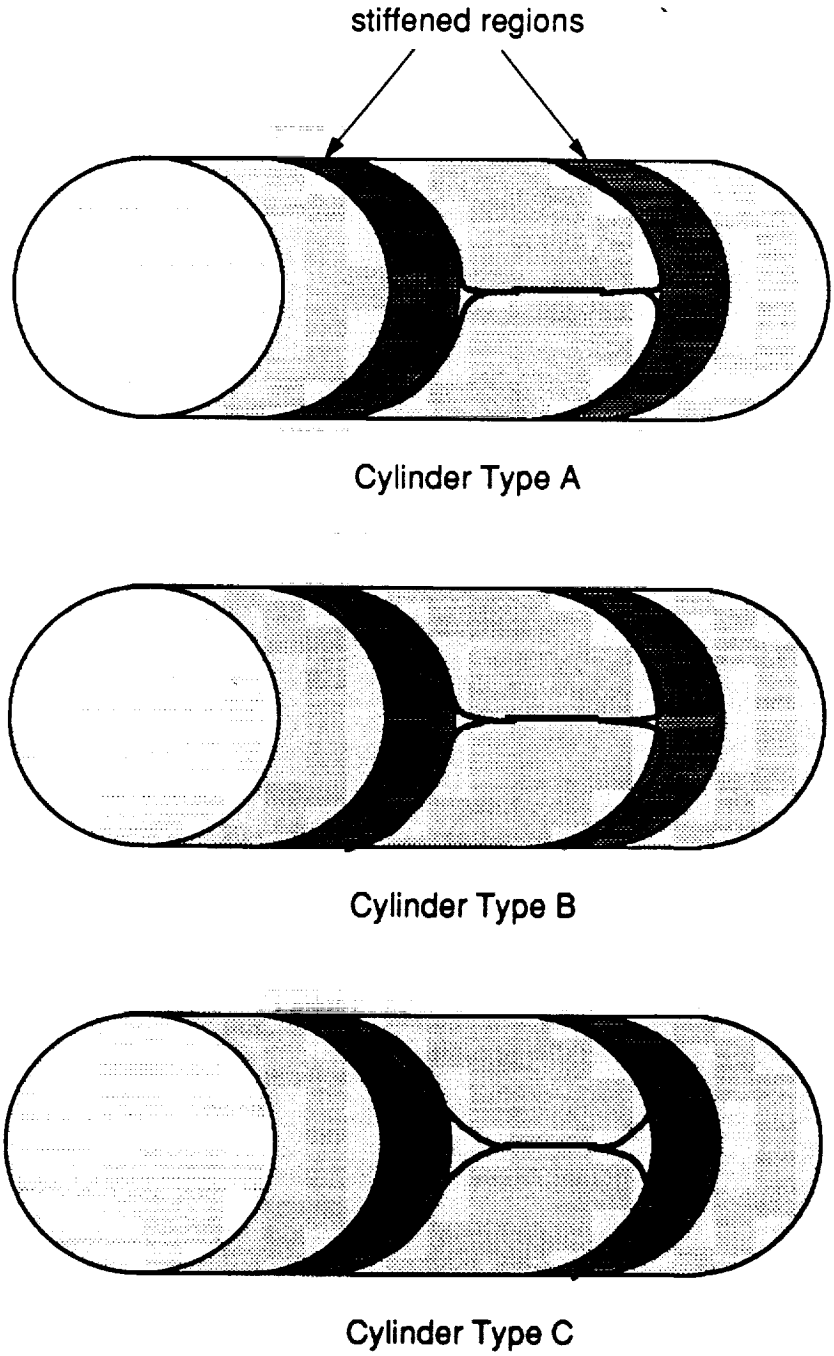

Figure 5 Schematic of damage propagation paths in cylinders types C, D, and E with 51 mm long slits

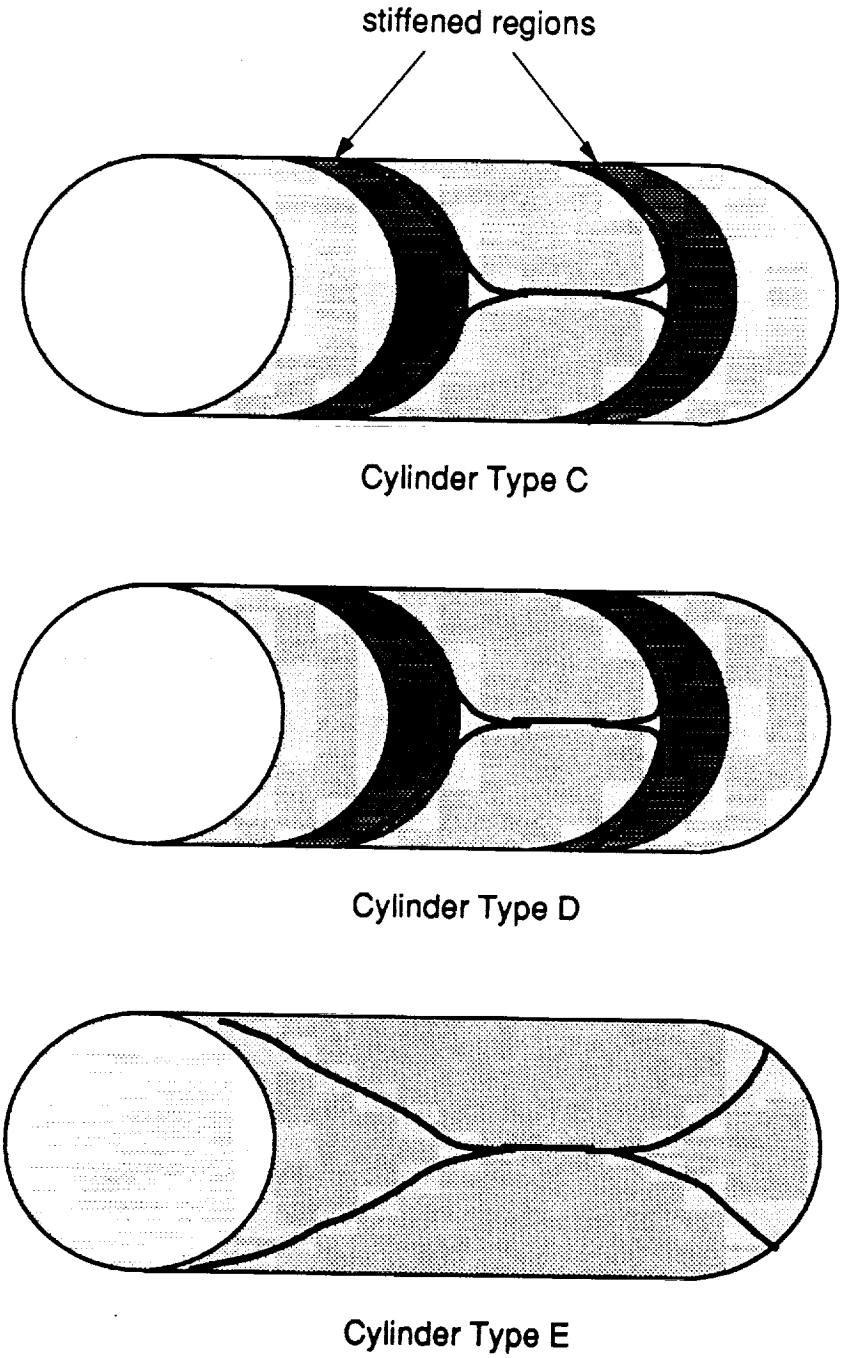

Figure 6 Edge-on view of layups illustrating the asymmetric nature of the manufactured specimen.

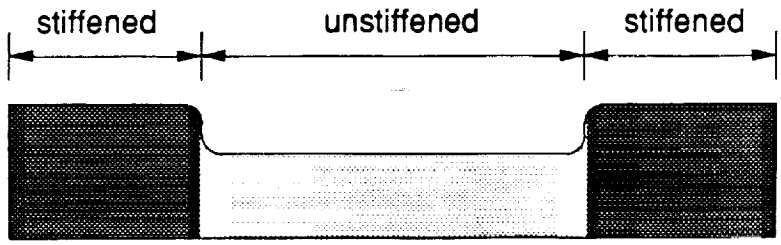

Side view of laminate, showing
stiffened and unstiffened regions

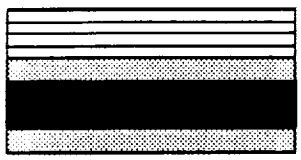

Stiffened Region for
Specimen Type A

Stiffened Region for
Specimen Type B

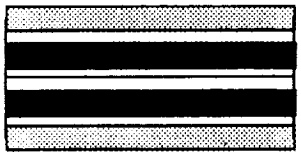

Stiffened Region for
Specimen Type C

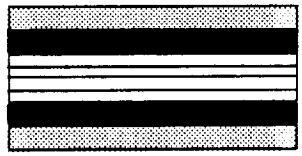

Stiffened Region for
Specimen Type D

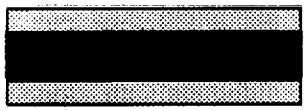

Unstiffened Region

0 degree fabric ply

45 degree fabric ply

tape stiffener ply

Figure 7 Photograph and computer enhanced image of photoelastic test result for panel A1 at far-field longitudinal strain of 3000 microstrain

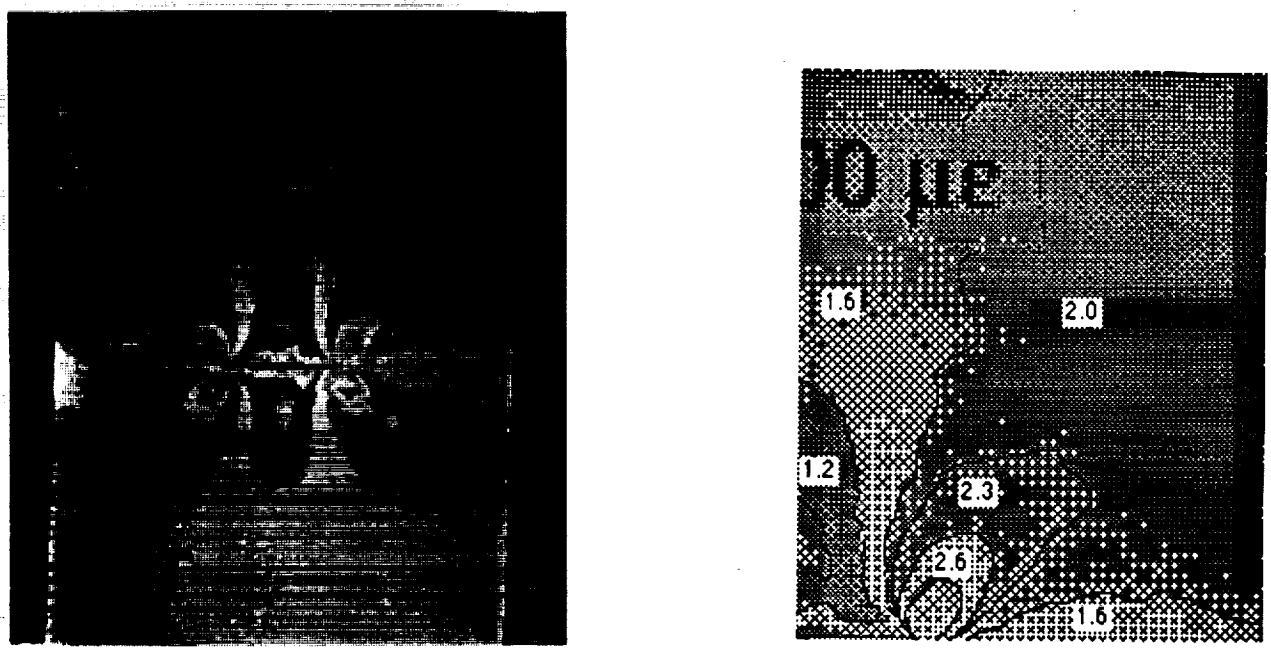

Figure 8 Photograph and computer enhanced image of photoelastic test result for panel B1 at far-field longitudinal strain of 3000 microstrain

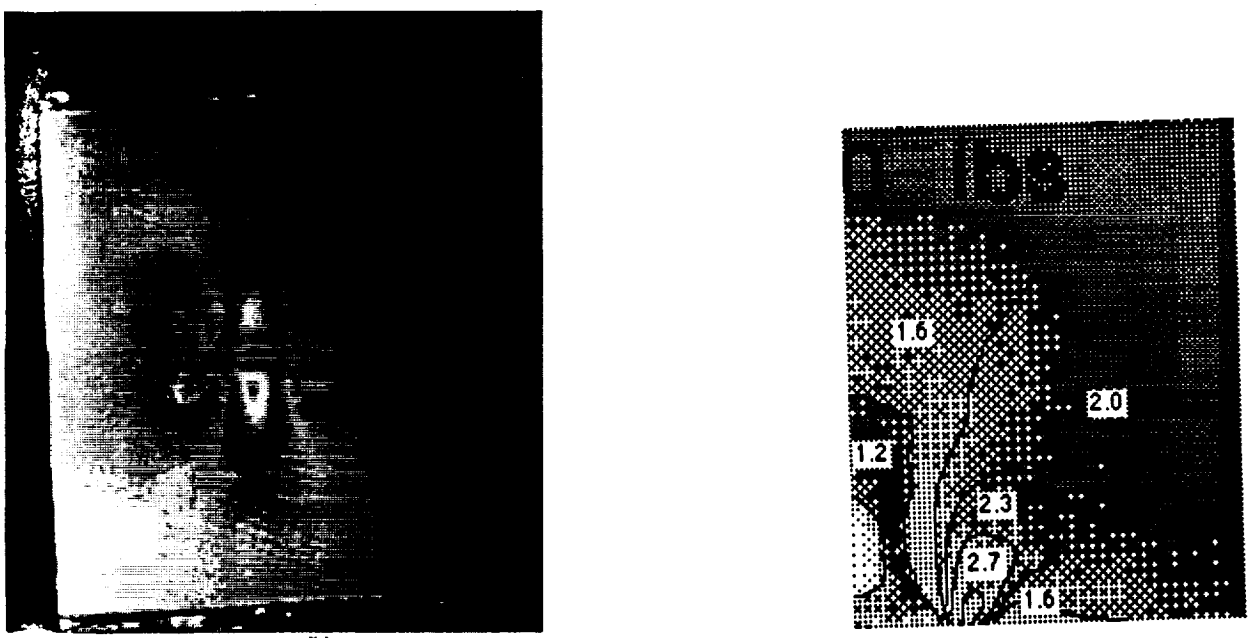

Figure 9 Photograph and computer enhanced image of photoelastic test result for panel C1 at far-field longitudinal strain of 3000 microstrain

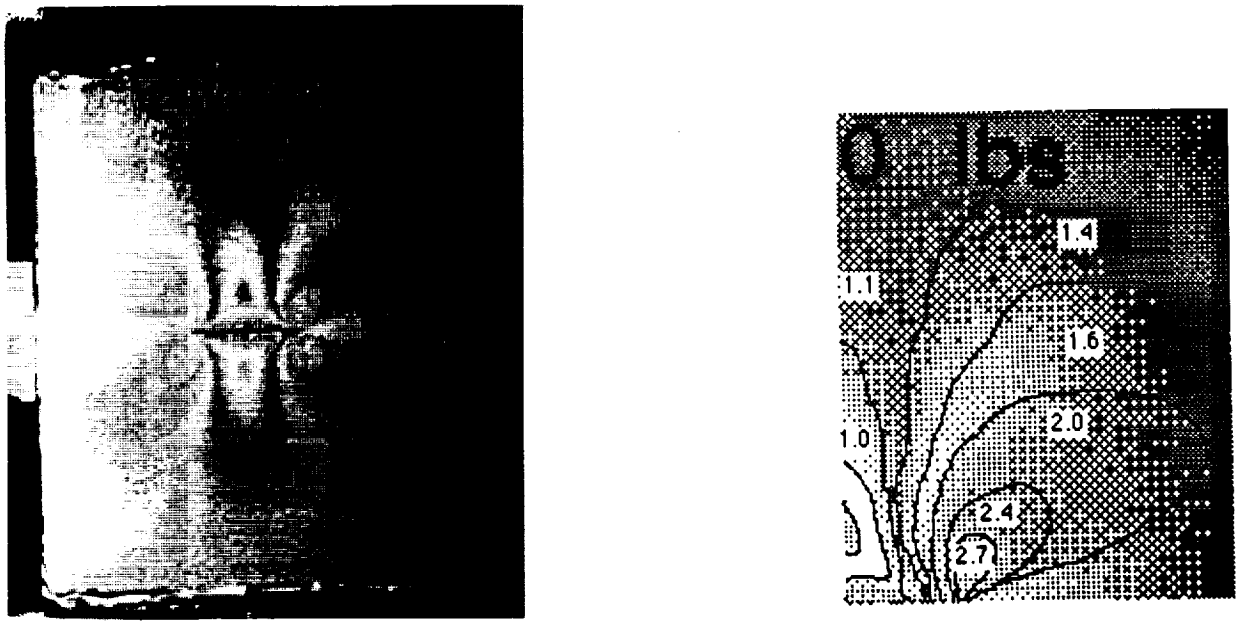

Figure 10 Analytical prediction of photoelastic patterns for panels A1, B1, and C1 at far-field longitudinal strain of 3000 microstrain

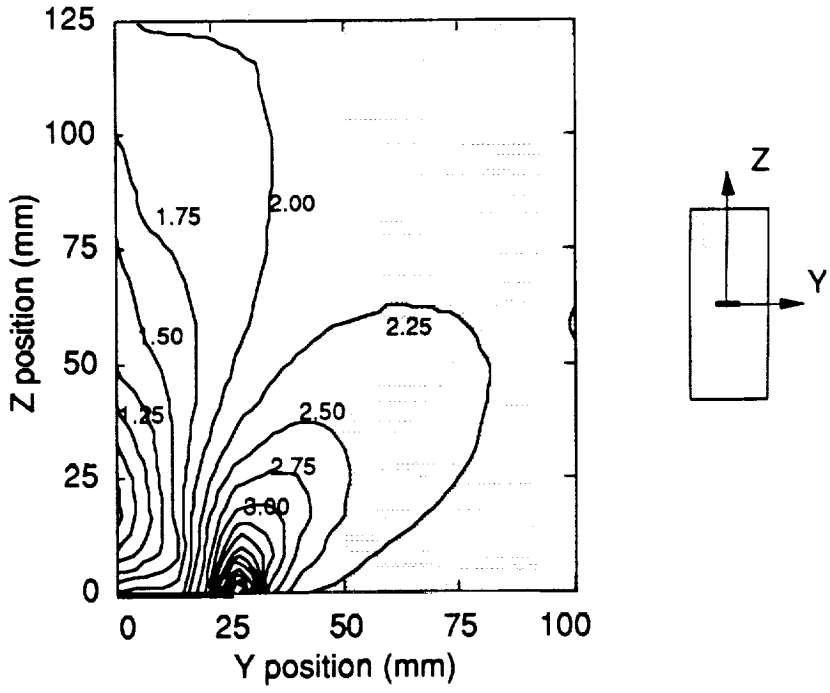

Figure 11 Normalized maximum tensile strain for panel with slit tip near stiffener

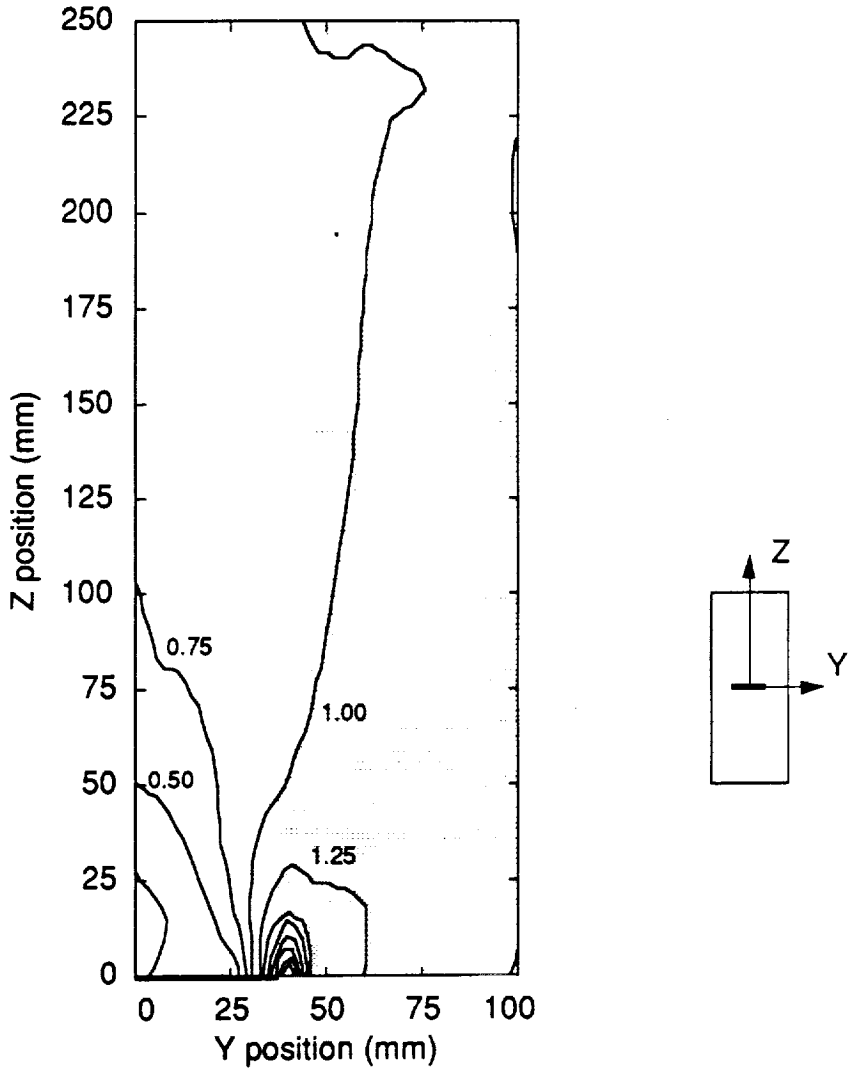

Figure 12 Orientation of maximum tensile strain for panel with slit tip near stiffener

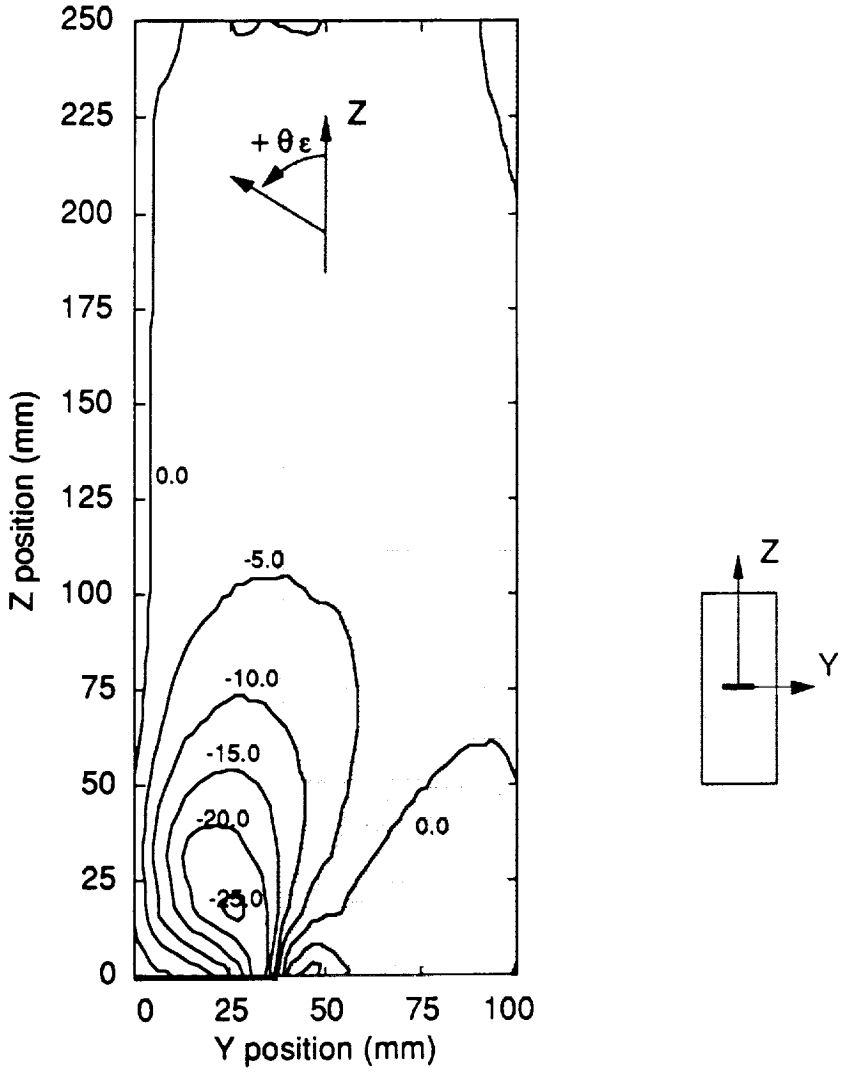

Figure 13 Normalized maximum tensile strain for stiffened cylinder with 225.mm long slit

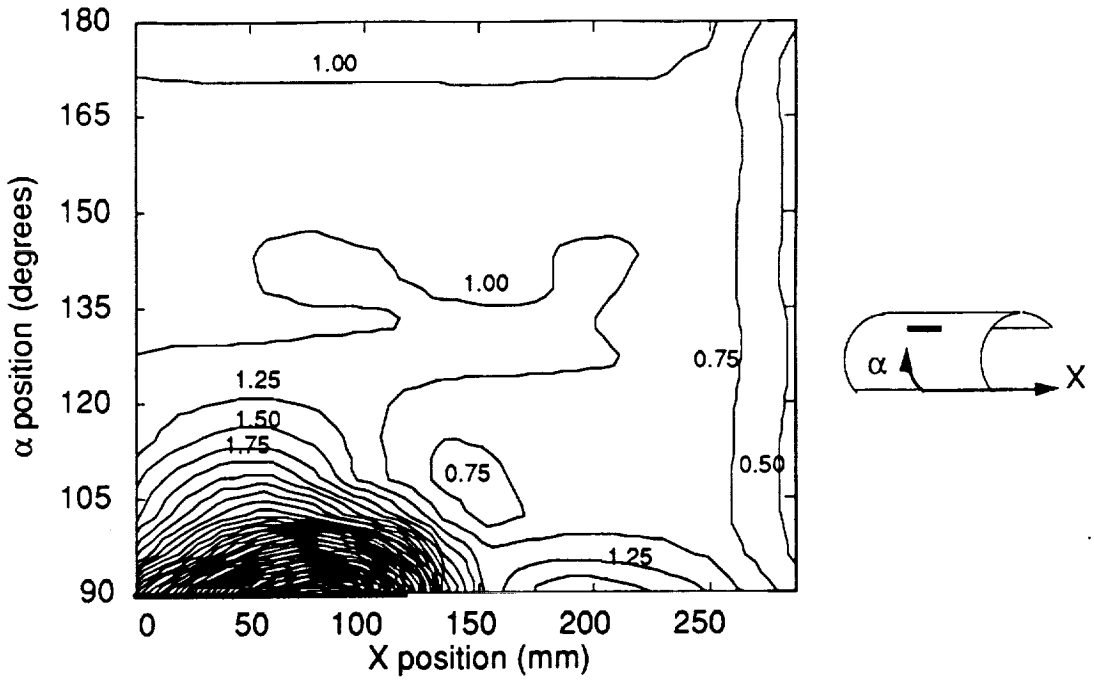

Figure 14 Normalized maximum tensile strain for unstiffened cylinder with 225 mm long slit

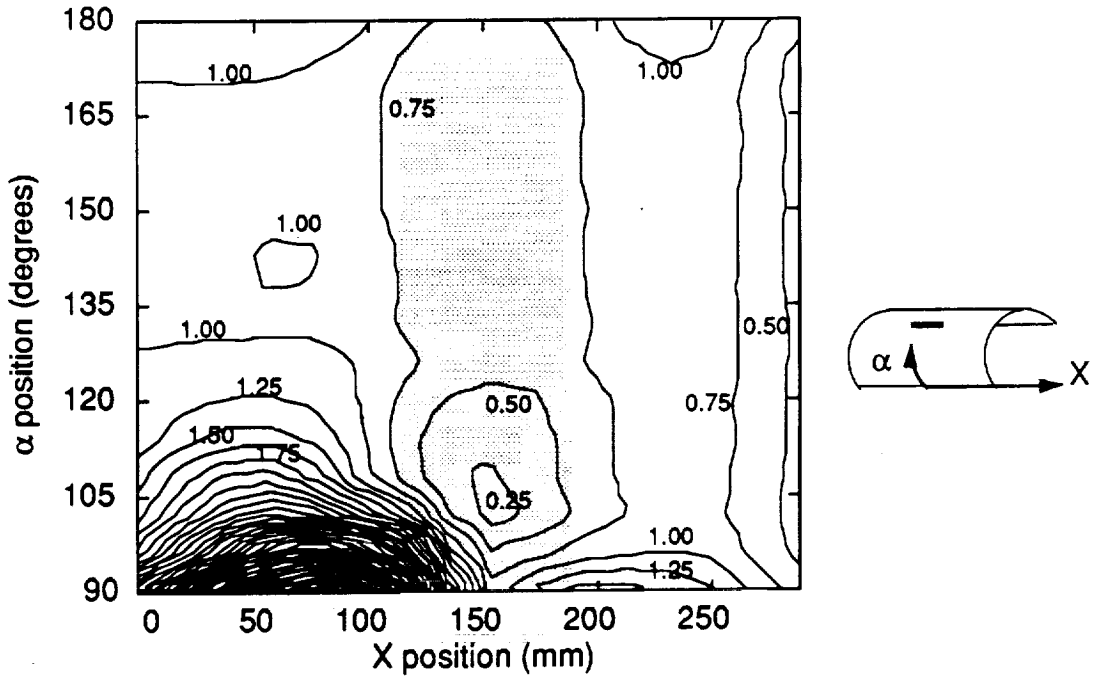

Figure 15 Orientation of maximum tensile strain for unstiffened cylinder with 225 mm long slit

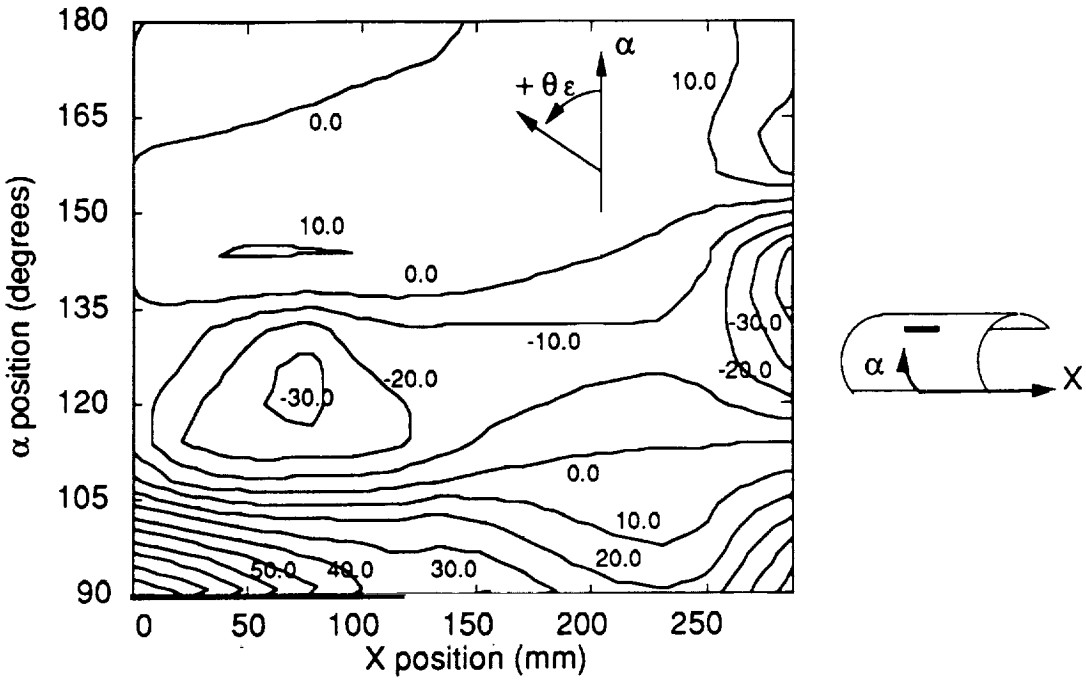

Figure 16 Orientation of maximum tensile strain for stiffened cylinder with 225 mm long slit

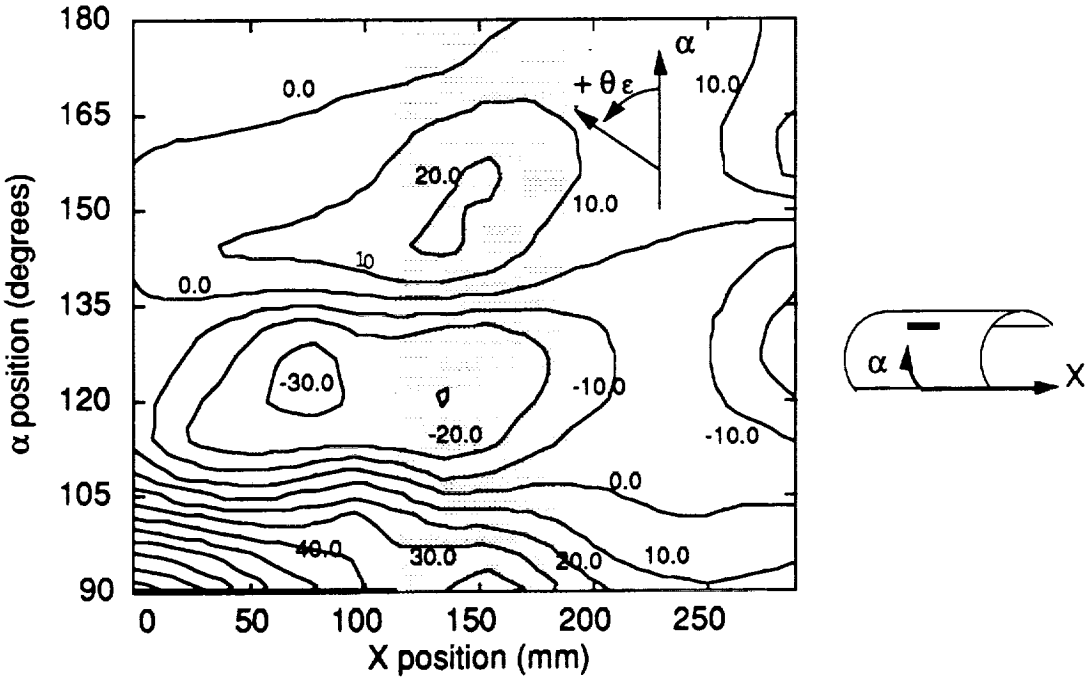

Table 1 Specimen Type and Failure Data for Plate Specimens

Plate Type*	Stiffener Width (mm)	Slit Length, 2a (mm)	Failure Load (kN)	Failure Stress (MPa)
A1	48	51	108.14	249.66
A2	48	102	103.02	237.84
A3	64	71	156.20	332.12
B1	48	51	118.82	274.32
B2	48	102	99.68	230.13
B3	64	71	129.05	274.37
C1	48	51	113.92	263.00
C2	48	102	76.32	176.20
C3	64	71	113.48	241.29

*All specimens have the same base laminate, $[0_f/45_f]_S$. Stiffener layups are:

Specimen Designation	Stiffener Layup
A	$[0_4/(0_f/45_f)_S]T$
B	$[0_2/0_f/45_f]_S$
C	$[0_f/0/45_f/0]_S$

0 represents a single ply of AS4/3501-6 unidirectional tape stiffener

0_f represents a single ply of 0-degree A370/3501-6 five harness weave fabric

45_f represents a single ply of 45-degree A370/3501-6 five harness weave fabric

Table 2 Specimen Type and Failure Data for Cylinders

Cylinder Number	Specimen Type	Cylinder Length (mm)	Slit Length, 2a (mm)	Failure Pressure (MPa)	Failure Hoop Stress (MPa)	Length of Damage at Bifurcation (mm)
1	A	610	102	0.556	60.57	216
2	B	610	102	0.774	84.31	210
3	C	610	102	0.604	65.79	133
4	A	610	178	0.389	42.37	178
5	B	610	165	0.396	43.14	165
6	C	610	51	1.320	143.79	159
7	E*	610	51	1.160	126.36	197
8	C	711	52	1.110	120.91	191
9	D	610	52	1.039	113.18	197

*All specimens have the same base laminate, $[0_f/45_f]_S$. Stiffener layups are:

Specimen Designation	Stiffener Layup
A	$[0_4/(0_f/45_f)_s]T$
B	$[0_2/0_f/45_f]_s$
C	$[0_f/0/45_f/0]_s$
D	$[0_f/45_f/0_2]_s$
E	None

0 represents a single ply of AS4/3501-6 unidirectional tape stiffener

0_f represents a single ply of 0-degree A370/3501-6 five harness weave fabric

45_f represents a single ply of 45-degree A370/3501-6 five harness weave fabric